Endogenous Sonic Hedgehog limits inflammation and angiogenesis in the ischaemic skeletal muscle of mice

Caroline Caradu, Alexandre Guy, Chloé James, Annabel Reynaud, Alain-Pierre Gadeau, Marie-Ange Renault

Endogenous Sonic Hedgehog limits inflammation and angiogenesis in the ischaemic skeletal muscle of mice

Caroline Caradu, Alexandre Guy, Chloé James, Annabel Reynaud, Alain-Pierre Gadeau, Marie-Ange Renault

Article title

Endogenous Sonic Hedgehog limits inflammation and angiogenesis in the ischemic skeletal muscle of mice

Short title
Endogenous Shh limits angiogenesis

Authors' names and affiliations

Caroline Caradu, MD[1], Alexandre Guy, MD[1], Chloé James, MD, PhD[1], Annabel Reynaud[1], Alain-Pierre Gadeau, PhD[1] and Marie-Ange Renault, PhD[1]

[1] Univ. Bordeaux, Inserm, Biology of Cardiovascular Diseases, U1034, CHU de Bordeaux, F-33604 Pessac, France

Corresponding Author
Marie-Ange Renault
INSERM U1034
1, avenue de Magellan
33604 Pessac
France
e-mail : marie-ange.renault@inserm.fr
Tel : (33) 5 57 89 19 79
Fax : (33) 5 56 36 89 79

Keywords:
Ischemia, Angiogenesis, Sonic Hedgehog, Macrophages, endothelial cells

Abstract

Aims:

Hedgehog (Hh) signalling has been shown to be re-activated in ischaemic tissues and participate in ischaemia-induced angiogenesis. Sonic Hedgehog (Shh) is upregulated by more than 80-fold in the ischaemic skeletal muscle, however its specific role in ischaemia-induced angiogenesis has not yet been fully investigated. The purpose of the present study was to investigate the role of endogenous Shh in ischaemia-induced angiogenesis.

Methods and results:

To this aim, we used inducible Shh knock-out (KO) mice and unexpectedly found that capillary density was significantly increased in re-generating muscle of Shh deficient mice 5 days after hind limb ischaemia was induced, demonstrating that endogenous Shh does not promote angiogenesis but more likely limits it. Myosin and MyoD expression were equivalent in Shh deficient mice and control mice, indicating that endogenous Shh is not required for ischaemia-induced myogenesis. Additionally, we observed a significant increase in macrophage infiltration in the ischaemic muscle of Shh deficient mice. Our data indicate that this was due to an increase in chemokine expression by myoblasts in the setting of impaired Hh signalling, using tissue specific Smoothened conditional KO mice. The increased macrophage infiltration in mice deficient for Hh signalling in myocytes was associated with increased VEGFA expression and a transiently increased angiogenesis, demonstrating that Shh limits inflammation and angiogenesis indirectly by signalling to myocytes.

Conclusion:

Although ectopic administration of Shh has previously been shown to promote ischaemia-induced angiogenesis, the present study reveals that endogenous Shh does not promote ischaemia-induced angiogenesis. On the contrary, the absence of Shh leads to aberrant ischaemic tissue inflammation and a transiently increased angiogenesis.

1. Introduction

Ischemia, subsequent to artery obstruction in peripheral tissues, heart and brain, is responsible for half of the deaths in Europe and North America. While recent progress in medical treatments has led to increased survival and quality of life for patients, results remain inconsistent especially in aged and diabetic patients. The concept that new blood vessels can be grown to enhance tissue perfusion is now achieving widespread acceptance [1]. To date several pro-angiogenic factors, including vascular endothelial growth factor (VEGF) and fibroblast growth factors (FGFs), have been tested in human clinical trials as a complement or an alternative to surgical revascularization; however their effects remain limited [2]. Therefore, a better understanding of the underlying mechanisms involved in ischemic muscle revascularization may help to optimize future clinical interventions.

Embryonic signalling pathways, including the Hedgehog (Hh) pathway, provide promising new targets for angiogenic therapies [3, 4]. Indeed, previous investigations have reported that inhibition of Hh protein activity, by neutralizing 5E1 antibody administration, impairs ischemia-induced angiogenesis both in the setting of hind limb ischemia and myocardial infarction, in mice [5, 6]. Conversely, when Sonic Hedgehog (Shh), one of the Hh ligands, was administered either as a recombinant protein or via gene therapy, it promoted neovascularization of ischemic tissues by promoting both angiogenesis [7] and endothelial progenitor cell recruitment [8]. Studies conducted to elucidate cellular mechanisms responsible for these findings have shown that Shh induces overexpression of several proangiogenic growth factors, including VEGFA and Angiopoietin-1, by fibroblasts and cardiomyocytes [7, 8].

However, despite evidence for the *in vivo* effects of Hh signalling in adults, the molecular mechanisms by which endogenous Hh signalling contributes to ischemia-induced angiogenesis have yet to be fully elucidated. For instance, since the 5E1 antibody blocks activity of all three Hh ligands (Shh, Desert Hh (Dhh) and Indian Hh (Ihh)) [9] the specific role of each Hh protein in the regulation of blood vessel homeostasis has not yet been established. We recently demonstrated that Dhh is necessary to drive angiogenesis in ischemic skeletal muscle. Interestingly, investigation of its mechanism of action revealed that it does not modulate endothelial cell (EC) function directly; on the contrary, it promotes angiogenesis by maintaining peripheral nerve-derived angiogenic factors in the ischemic muscle [10].

The purpose of the present study was to investigate the specific role of endogenous Shh in ischemia-induced angiogenesis. Among the three Hh ligands, Shh expression has previously been demonstrated to be the most up-regulated in the setting of ischemia [7, 8, 10]; with previous reports indicating that Shh is upregulated up to 80 fold in ischemic skeletal muscle, 2 days after hind limb ischemia (HLI) is induced [10].

2. Methods

2.1. Mice

Shh Floxed (Shh^{Flox}) mice [11], Smo Floxed (Smo^{Flox}) mice [12], $Rosa26^{mTmG}$ mice [13], HSA-Cre^{ERT2} mice [14] and LysM-Cre mice [15] were obtained from Jackson Laboratories. Rosa26-Cre^{ERT2} mice [16] were obtained from the "Institut Clinique de la Souris" (Strasbourg, France). Pdgfb-Cre^{ERT2} mice [17] were kindly provided by M. Fruttiger.

Animal experiments were performed to conform to the guidelines from Directive 2010/63/EU of the European Parliament on the protection of animals used for scientific purposes, and approved by the local Animal Care and Use Committee of Bordeaux University (CEEA50).

Rosa26-Cre^{ERT2}, HSA-Cre^{ERT2} and LysM-Cre mice were genotyped using the following primers 5'-TAAAGATATCTCACGTACTGACGGTG-3' and 5'-TCTCTGACCAGAGTCATCCTTAGC-3' that amplify 493 bp of the Cre recombinase sequence. Pdgfb-Cre^{ERT2} mice were genotyped using the following primers 5'-CCAGCCGCCGTCGCAACT-3' and 5'-GCCGCCGGGATCACTCTCG-3'. Shh Floxed mice were genotyped using the following primers 5'-ATGCTGGCTCGCCTGGCTGTGGAA-5' and 5'-

GAAGAGATCAAGGCAAGCTCTGGC-3', Smo Floxed mice were genotyped using the following primers 5'-CCACTGCGAGCCTTTGCGCTAC-3' and 5'-CCCATCACCTCCGCGTCGCA-3' which amplifies a 446 bp fragment of the WT allele and 5'-CTTGGGTGGAGAGGCTATTC-3' and 5'-AGGTGAGATGACAGGAGATC-3' which amplifies 280 bp of the floxed allele. Rosa26^{mTmG} mice were genotyped using the three following primers 5'-CTCTGCTGCCTCCTGGCTTCT-3', 5'-CGAGGCGGATCACAAGCAATA-3', and 5'-TCAATGGGCGGGGGTCGTT-3'.
Cre recombinase, of Rosa26-Cre^{ERT2} and Pdgfb-Cre^{ERT2} mice, was activated by intraperitoneal injection of 1 mg tamoxifen for 5 consecutive days starting one week before HLI surgery was performed. (i.e.: from day -7 to day -3 before surgery). Cre recombinase of HSA-Cre^{ERT2} mice was activated by intraperitoneal injection of 1 mg tamoxifen for 10 consecutive days starting the day HLI surgery was performed (i.e.: from day 0).

2.2. HLI model and assessments

HLI was induced by ligation and resection of the left femoral artery, as previously described [10, 18].
Briefly, mice were anesthetized with isoflurane, aseptically prepared and a 5 mm incision was made in the left thigh region. Two ligations were made around the femoral artery, at the proximal end of the femoral artery and the distal portion of the saphenous vein. The femoral artery and all side-branches were then dissected and excised. The connective tissues were closed with interrupted 6-0 absorbable sutures. To minimize pain caused by the surgery, mice were administered intraperitoneally with 0.05 mg/kg buprenorphin 30 minutes before and 8 hours after surgery.
Mice were sacrificed by cervical dislocation at the indicated time points.
For histological assessment and gene expression analysis, tibialis anterior muscle was harvested, and cut in half. The lower half was fixed in methanol, paraffin-embedded, and cut into 6-µm sections, and the upper half was snap frozen in liquid nitrogen.
Foot perfusion was measured using a MoorLDI2-IR apparatus after mice were anesthetized by intraperitoneal injection of ketamine (100 mg/kg) and xylazine (10 mg/kg), and reported as the ratio of blood perfusion in the ischemic vs non-ischemic limb.
Micro-CT vasculature imaging was performed as previously described [19]. More precisely, mice euthanized by a lethal injection of pentobarbital, were perfused via the ventral aorta first with a heparinized isotonic solution and then with a 10% Formalin solution, followed by a mixture of 88% Neoprene latex (Neoprene Latex Dispersion 671 A, Dupont, France) and barium sulphate (0.08 g/mL, MicrOpaque® oral solution, Guerbet, France). Next, the mouse was put into acid solution for the latex to harden, then, after dissection; the organs were fixed overnight in 10% Formalin at 4°C. For mCT scanner data processing and analysis, we used the Skyscan1174 Micro-CT scanner from Bruker with spatial resolution of 6 to 30 µm, with the Skyscan® and NRecon® programs. Voltage parameters were 48 kV with a mean current of 805 µA. Our acquisition protocol consisted of 360 views with 5 averaged images per position, with a voxel volume of 17 µm^3. 3D images were obtained using the IMARIS® program.

2.3. Immunostaining and quantifications

ECs were identified with rat anti-CD31 antibodies (BD Pharmingen Inc). Myocytes were identified using rabbit polyclonal anti-Desmin antibodies (Millipore), leucocytes were identified using rat anti-CD45 antibodies (BD Pharmingen Inc), neutrophils were identified using rat anti-Ly6G (GR1) antibodies (BD Pharmingen Inc) and macrophages were identified using rat anti-CD68 antibodies (Biolegend). VEGFA was stained using rabbit anti-VEGFA antibodies (Abcam). GFP was identified using rabbit anti-GFP antibodies (Molecular probe). For immunofluorescence analyses, primary antibodies were resolved with Alexa-Fluor–conjugated secondary antibodies (Invitrogen) and nuclei were counterstained with DAPI (1/5000). For immunohistochemical analyses, primary antibodies were sequentially stained with biotin-conjugated secondary antibodies (Vector Laboratories) and streptavidin-HRP complex (Amersham), then the stain was developed with a DAB substrate kit (Vector Laboratories); tissues were counterstained with hematoxylin.

Capillary, neutrophil and macrophage density was evaluated in sections stained for the expression of CD31, GR1 and CD68, respectively. For each muscle section, CD31+ vessels, GR1+ neutrophils and CD68+ macrophages were counted in 20 pictures randomly taken under 40x magnification. One section was quantified per muscle (per mouse) because we verified muscle repair is relatively uniform along the length of the tibialis anterior muscle. Myogenesis was assessed after Desmin staining of muscle sections as the percentage of Desmin+ area. Only mice, in which there was histologic evidence of ischemia in the tibialis anterior muscle, as assessed by hematoxylin and eosin (H&E) staining, were included in the study.

2.4. Plasmids/Gene Therapy

Gene therapy was performed in 12 week old mice. Immediately after HLI surgery was performed, mice were randomly assigned to receive 200 µg pIRES-EGFP or 200 µg pIRES-NShh [10] together with 0.05% pluronic. The DNA/pluronic mix was injected intramuscularly in the tibialis anterior muscle as previously described [10]. Mice scheduled to be sacrificed at day 5 were injected immediately after surgery while mice scheduled to be sacrificed at day 10 were injected both at day 0, immediately after surgery, and at day 4.

2.5. Flow cytometry

The ischemic tibialis anterior muscle was subsequently dissociated in 2 mg/mL type 4 collagenase (Wortgingthon) for 1 hour at 37°C and filtered on a 40 µm strainer. Macrophages were labelled with PE-conjugated anti-CD11b (Biolegend) and FITC-conjugated anti-CD11c (Biolegend) antibody, before they were counted using a ACCURI® C6 flow cytometer (BD). Neutrophils were labelled with APC conjugated anti-Ly6G and Ly6C (BD Pharmingen Inc).

2.6. Quantitative RT-PCR

RNA was isolated using Tri Reagent® (Molecular Research Center Inc) as instructed by the manufacturer, from $3x10^5$ cells or from skeletal muscle that had been snap-frozen in liquid nitrogen and homogenized. For quantitative RT-PCR analyses, total RNA was reverse transcribed with M-MLV reverse transcriptase (Promega) and amplification was performed on a DNA Engine Opticon®2 (MJ Research Inc) using B-R SYBER® Green SuperMix (Quanta Biosciences). Primer sequences are reported in Supplementary table 1.

The relative expression of each mRNA was calculated by the comparative threshold cycle method and normalized to HPRT mRNA expression.

2.7. Cell culture

Both C2C12 cells (ATCC) and RAW 264.7 macrophages (ATCC) were cultured in DMEM containing 4.5 g/L glucose and supplemented with 10% fetal bovine serum. Before any treatment, cells were serum starved in 0.5% fetal bovine serum containing culture medium for 24 hours.

Primary cultured myoblasts were isolated from $Smo^{Flox/Flox}$ mice or their WT littermates as previously described [20]. Briefly, to isolate myoblasts, mouse limb skeletal muscle was dissociated in 2.4 U/mL dispase (Sigma) and 1.5 mg/mL collagenase 2 (Worthington) containing culture medium for 20 minutes at 37°C. Muscle cells were then seeded on 50 µg/mL type I collagen coated dishes (Sigma) and cultured in 20% FBS containing HAM F10 nutrient mixture. Round shape cells (i.e. myoblasts) were enriched, and fibroblasts were eliminated by passaging cells with PBS that contained no trypsin. To preserve a proliferating phenotype, myoblasts were maintained in culture medium containing 50% HAM F10 nutrient mixture and 50% DMEM, supplemented with 20% FBS and, FGF2 (2.5 ng/mL). Both $Smo^{Flox/Flox}$ and WT myoblasts were transduced with Cre-expressing lentiviruses [20] at a MOI of 20.

2.8. Migration assay

Cell migration was evaluated by using a modified Boyden's chamber (Neuro Probe, Inc). Briefly, a polycarbonate filter (8-µm pore size) (GE Infrastructure) was coated with a solution containing 0.1% gelatin (Sigma-Aldrich) and inserted between the upper and lower wells. Cells, 5×10^4 per well, were seeded in the upper chamber, and the lower chamber contained myoblast-conditioned medium containing 2 µg/mL Ccl2 blocking antibodies (R&D systems) or isotype control. Migration was evaluated as the mean number of migrated cells in 3 high-power fields (HPF) (20× magnification) per well.

2.9. Phagocytosis Assay

Five x 10^4 RAW 264.7 macrophages were seeded in each well of a 24 well plate. After cells were serum-starved in 0.5% fetal bovine serum containing culture medium for 24 hours, they were treated with or without 1 µg/mL recombinant N-Shh (Shenandoah) or 30 nM GDC-0449 (Sigma) for 24 hours. The media was then removed from cells and replaced by fresh media containing 40 FITC-labelled Zymosan A Bioparticles (Molecular Probes™)/cells. After 1 hour incubation at 37°C, cells were washed with ice-cold PBS and fixed with 10% Formalin. Nuclei were stained with DAPI. Phagocytosis was quantified as the ratio of FITC positive surface area over the number of DAPI positive nuclei. Phagocytosis was evaluated in 3 high-power fields (HPF) (20× magnification) per well.

2.10. Statistics

Results are reported as mean ± SEM. Comparisons between groups were analysed for significance with the non-parametric Mann-Whitney test or with a one way ANOVA analysis followed by a Bonferroni's multiple comparison test when there were 3 or more groups to compare. Differences between groups were considered significant when $p<0.05$. *: $p<0.05$; **: $p<0.01$; ***: $p<0.001$.

3. Results

3.1. Endogenous Shh does not promote ischemia-induced angiogenesis.

To investigate the role of endogenous Shh in ischemia-induced angiogenesis, we created Shh inducible knock out (iKO) adult mice. To this aim, we bred Shh conditional KO mice (Shh^{Flox}) with mice expressing the tamoxifen-inducible Cre ubiquitously (Rosa26-Cre^{ERT2} mice). We first assessed Cre recombinase activity in the skeletal muscle of adult mice, by breeding Rosa26-Cre^{ERT2} mice with $Rosa26^{mTmG}$ mice. Recombination of the $Rosa26^{mTmG}$ allele was verified after GFP staining of skeletal muscle sections (Figure 1A). Additionally, effective Shh knock-down was verified by measuring Shh mRNA expression in the ischemic and non-ischemic skeletal muscle of Rosa26-Cre^{ERT2}; $Shh^{Flox/Flox}$ mice. As shown Figure 1B, Shh mRNA expression was reduced by approximately 85% while Dhh and Ihh mRNA expression was not modulated (Figure 1B-D).

Rosa26-Cre^{ERT2}; $Shh^{Flox/Flox}$ (Shh iKO) and control $Shh^{Flox/Flox}$ mice then underwent HLI surgery. Revascularization of the ischemic leg was evaluated, 5 and 10 days after surgery, by measuring capillary density in the ischemic tibialis anterior muscle and foot perfusion. Unexpectedly, we found that capillary density was significantly increased in Shh deficient mice compared to control mice 5 days after HLI surgery was performed (Figure 1E-F). However, 10 days after surgery, capillary density was equivalent in both groups. Similarly, foot perfusion increased in Shh deficient mice compared to control mice 5 days after HLI surgery. Foot perfusion was equivalent in both groups at day 10 post-surgery, consistent with capillary density data (Figure 1G-H).

Altogether these results demonstrate that Shh deficiency leads to a transiently increased angiogenesis in the ischemic skeletal muscle however; this response appears to be inefficient and does not lead to a long-lasting improved foot perfusion. Because this result was unexpected and contrary to previous reports, we administered Shh ectopically via gene therapy (Figure 2A-B), in both Shh deficient mice and their control littermates, to confirm that we were able to reproduce results from the literature [6, 7]. As shown Figure 2C and 2D, Shh gene therapy significantly increased capillary density in control mice both at day 5 and at day 10, which is fully consistent with previous studies [7, 8,

[21] and confirms that, when administered ectopically, Shh is pro-angiogenic. Blood flow was significantly increased at day 5, nevertheless, this effect was no longer observable at day 10 (Figure 2E-F). Notably, capillary density was increased by 2 fold at day 5 while it was only increased by 1.5 fold at day 10. However, Shh gene therapy had no effect in Shh deficient mice in which capillary density was already high. In summary, ectopic administration of Shh did not rescue the phenotype of Shh deficient mice, suggesting that endogenous and exogenous Shh have different effects.

Therefore our data demonstrates that in contrast to Dhh [10], endogenous Shh does not promote ischemia-induced angiogenesis, and more likely attenuates the angiogenesis process.

3.2. Endogenous Shh is necessary for new capillary muscularization but not arteriogenesis.

Shh has been shown to be involved in blood vessel muscularization [22], as such, we measured smooth muscle cell coverage of newly formed capillaries within the ischemic muscle of Shh deficient mice and control mice. We found that the percentage of smooth muscle myosin heavy chain (smMHC) positive capillaries was significantly decreased in the absence of Shh, both 5 and 10 days after HLI was induced (Figure 3A-B), demonstrating that in the absence of Shh, angiogenesis is transiently increased but the newly formed capillaries remain immature.

This latter result is consistent with previous literature reports [7, 21, 22], and further confirms the essential role of Shh in blood vessel maturation.

In addition, we evaluated the role of Shh in arteriogenesis using micro CT imaging. To do so, Shh iKO mice and their control littermates underwent HLI surgery. Five days later, mice were sacrificed and perfused with a barium/Latex mixture through the aorta. As shown in Figures 3C-E, collateral formation (i.e. collateral number and collateral diameter) were equivalent in Shh deficient and control mice, showing that endogenous Shh does not participate in collateral formation in the setting of ischemia.

3.3. Endogenous Shh is not necessary for ischemia-induced myogenesis.

Since Hh signalling is also known to participate in adult myogenesis [23], we evaluated myogenesis in Shh deficient mice and their control littermates. Ten days after HLI surgery, the surface area of ischemic muscle recolonized by new muscle fibers (desmin + with central nuclei) was the same in Shh iKO mice and in control mice (Supplemental Figure 1A-B). Moreover, the expression profile of MyoD, an early marker of myogenesis (Supplemental Figure 1C), and Myh1, a late marker of myogenesis, (Supplemental Figure 1D) were not different in the absence of Shh, demonstrating that Shh is not necessary for ischemia-induced myogenesis.

3.4. Shh limits macrophage recruitment in the ischemic muscle

Since Shh is strongly over expressed 2 days after HLI surgery, and its expression is back to baseline at day 5 [10], we tested the role of Shh in early events, such as inflammation, following ischemic injury.

To evaluate the impact of Shh KO on ischemic muscle inflammation, both Shh iKO mice and their control littermates underwent HLI surgery, and neutrophil infiltration was evaluated 2 days later. As shown in Figures 4A and 4B, GR1+ neutrophil infiltration was not different in the presence or absence of Shh. This result was confirmed by FACS analysis of Ly6G, Ly6C positive cells (Figure 4C). In contrast, when we assessed macrophage infiltration, which typically peaks 5 days after ischemia is induced, we found that CD68+ macrophage density in the ischemic muscle was significantly increased in Shh deficient mice (Figure 4D-E), demonstrating that Shh limits macrophage recruitment. Similarly, the number of CD11b, CD11c double positive cells within the ischemic muscle was significantly increased in Shh-deficient mice (Figure 4F).

Taken together these data demonstrate that Shh exhibits an anti-inflammatory action in ischemic tissue by limiting macrophage recruitment.

3.5. Shh does not limit macrophage recruitment by targeting macrophages directly.

To better understand how Shh limits macrophage infiltration in the ischemic muscle, we investigated the Shh-target cell type responsible for this effect. To do so, we used Smoothened conditional KO mice (Smo^{Flox}). Because Smoothened (Smo) is an essential positive regulator of Hh signalling, Smo^{Flox} mice are classically used to disrupt Hh signalling in specific cell types[12].

Smo KO was induced in inflammatory cells (macrophages and neutrophils) by breeding Smo^{Flox} mice with LysM-Cre mice. We first verified that Cre recombinase was expressed and active in neutrophils and macrophages infiltrating into the ischemic skeletal muscle of adult mice, by breeding LysM-Cre mice with $Rosa26^{mTmG}$ mice (Supplemental Figure 2).

LysM-Cre; $Smo^{Flox/Flox}$ and their control littermates underwent HLI surgery. Macrophage density was evaluated by immunohistochemistry and flow cytometry. Both the number of CD68+ cells counted on muscle cross sections (Supplemental Figure 3A-B) and the number of CD11b, CD11c double positive cells counted by flow cytometry (Supplemental Figure 3C) were equivalent in LysM-Cre, $Smo^{Flox/Flox}$ mice and their control littermates, demonstrating that Shh does not limit macrophage recruitment by signalling to macrophages directly.

To further confirm this result, we performed *in vitro* assays using cultured macrophages. We first found that Shh recombinant protein had no effect on Gli1 or Gli2 mRNA expression (Supplemental Figure 4A-B). Nevertheless, macrophages were sensitive to some autocrine-induced Hh signalling through Gli2 (Supplemental Figure 4B), since inhibition of Smo with GCD-0449 significantly decreased Gli2 mRNA expression. Consistent with *in vivo* data, neither Shh treatment nor Smo inhibition modulated chemokine expression, including Ccl2 or Ccl5 (Supplemental Figure 4C-D), or macrophage migration (Supplemental Figure 4E). In addition, Hh signalling had no effect on macrophage phagocytic activity (Supplemental Figure 4F). Finally, we tested whether Shh or GDC-0449 would modulate VEGFA expression, and found they did not (Supplemental Figure 4G). Accordingly, capillary density was not increased in LysM-Cre; $Smo^{Flox/Flox}$ mice in comparison to their control littermates (Supplemental Figure 5A-B). Nevertheless, we observed a significant decrease in capillary density at day 5 in LysM-Cre; $Smo^{Flox/Flox}$ mice which was associated with improved muscle perfusion 10 days after HLI surgery was performed (Supplemental Figure 5C-D). This phenotype is more likely independent of Shh, since it is not recapitulated in Shh deficient mice.

3.6. Shh does not limit macrophage recruitment by modulating EC phenotype

We next tested whether Shh limits macrophage density in ischemic muscle by modulating the EC phenotype. EC are active players of macrophage recruitment through the expression of adhesion molecules for inflammatory cells. Smo deletion in ECs was achieved using Pdgfb-Cre^{ERT2} mice, as previously described [10]. Macrophage infiltration was evaluated in the ischemic muscle in Pdgfb-Cre^{ERT2}; $Smo^{Flox/Flox}$ and control mice 5 days after HLI surgery, and Smo depletion in ECs did not lead to significant changes in macrophage density within the ischemic muscle (Supplemental Figure 6A-B). Consistent with this, flow cytometry data showed that the number of CD11b, CD11c double positive cells was equivalent in both genotypes (Supplemental Figure 4C). This result demonstrates that Shh does not limit macrophage recruitment by modulating the EC phenotype.

Notably, we previously reported that neither capillary density nor blood flow recovery were modified in Pdgfb-cre^{ERT2}; $Smo^{Flox/Flox}$ mice [10].

3.7. Hh signalling limits chemokine expression in myocytes.

Finally, we specifically disrupted Smo expression in myocytes, by breeding Smo^{Flox} mice with HSA-Cre^{ERT2} mice. We previously verified that Cre recombinase was active in newly generated skeletal myocytes in ischemic skeletal muscle [20]. HSA-Cre^{ERT2}; $Smo^{Flox/Flox}$ mice and their control littermates underwent HLI surgery. CD68 staining of ischemic muscle sections demonstrated that macrophage density was significantly increased in mice in which Smo expression had been specifically disrupted in myocytes (Figure 5A-B). This result was confirmed by flow cytometry analysis of CD11b, CD11c double positive cells (Figure 5C).

Together these results demonstrate that Shh does not limit macrophage recruitment in skeletal muscle by modulating inflammatory cells directly or the EC phenotype, but through its action on myocytes.

To further understand how Shh limits macrophage recruitment, we performed *in vitro* experiments using the C2C12 myoblast cell line. We found that inhibition of Hh signalling, with the Smo inhibitor GDC-0449, significantly increased expression of several cytokines that are chemotactic for macrophages, including Ccl2 and Ccl5 (Figure 5D-E). We confirmed these results in primary cultured myoblasts isolated from $Smo^{Flox/Flox}$ mice or $Smo^{+/+}$ control mice and subsequently transduced with Cre encoding lentivirus (Figure 5F-H).
To test whether Ccl2 produced by myoblasts can promote macrophage migration, we used conditioned medium from control and Smo KO myoblasts in which Ccl2 had or had not been blocked with anti-Ccl2 antibodies. We found that macrophage migration was significantly increased by Smo KO myoblast conditioned medium compared to control myoblast conditioned medium, and that Ccl2 blockage inhibited Smo KO myoblast-conditioned medium induced macrophage migration (Figure 5I).

These results demonstrate for the first time that endogenous Shh limits macrophage recruitment in ischemic tissue by downregulating chemokine expression in muscle cells.

3.8. "hyperinflammation" induces a transient increase in angiogenesis in Hh deficient mice
Because macrophages are known to produce proangiogenic molecules including VEGFA, we evaluated angiogenesis in HSA-Cre^{ERT2}; $Smo^{Flox/Flox}$ mice. Consistent with results obtained in Shh deficient mice, we observed a significant increase in capillary density in ischemic skeletal muscle of HSA-Cre^{ERT2}; $Smo^{Flox/Flox}$ mice compared to their control littermates 5 days after HLI (Figure 6A-B), which resulted in a significant increase in foot perfusion 10 days after HLI (Figure 6C-D). The increased capillary density was associated with significantly increased VEGFA levels (Figure 6E-F) within the ischemic muscle.

4. Discussion

To our knowledge, the present study is the first to use specific tools (i.e. Shh deficient mice) to investigate the role of endogenous Shh in angiogenesis in adult mice. This study demonstrates that endogenous Shh does not promote ischemia-induced angiogenesis, on the contrary it reveals that angiogenesis is transiently increased in the absence of Shh (Figure 7). This result was unexpected based on previous literature which demonstrated that administration of exogenous Shh promoted ischemia-induced angiogenesis both in ischemic skeletal muscle and infarcted heart muscle [7, 8].
Studies conducted to date have investigated the role of endogenous Hh signalling in ischemic tissue repair, using non-specific tools such as the monoclonal antibody 5E1 which blocks activity of the three different Hh ligands (Shh, Ihh and Dhh) [6] or the Smo inhibitor Cyclopamine [24]. Moreover the results of these studies were inconsistent; since Pola et al. reported that Hh signalling blockage with 5E1 antibodies inhibited ischemia-induced angiogenesis, while Bijlsma et al reported that Hh signalling blockage with cyclopamine did not affect angiogenesis.
Notably, our results are consistent with embryonic studies. Indeed, while ectopic Shh overexpression in the roof plate of the spinal cord was shown to induce hypervascularization of neurectoderm [25], Chiang et al. did not observe any obvious vascular defects in Shh deficient embryos [26]. Consistent with this, Van Tuil et al. reported that the pulmonary vascular bed of Shh KO embryos was decreased, but appropriate to the decrease in airway branching [27]. In contrast, other Hh family members including Ihh, were shown to be necessary for the formation of the anterior aorta [28] and angiogenesis, especially in the yolk sac [29]

Additionally, this study reveals that Shh exerts an anti-inflammatory action in ischemic tissue. The role of Shh as a regulator of inflammation was first suggested through its role in the regulation of thymocyte differentiation [30, 31]. Nevertheless, the role of Hh signalling in the regulation of inflammation is still poorly understood, while *in vitro* studies suggest that Shh promotes the expression of several chemokines including Ccl2, Ccl20, Cxcl1, Cxcl2 and Cxcl16 [32, 33]; studies performed in mice with impaired Hh signalling, have demonstrated that the loss of Hh signalling may lead to chronic tissue inflammation in the brain or intestine [34-36], or limit inflammation in *H Pylori* infected stomach [37]. Additionally, several pieces of evidence suggest that Hh signalling promotes Th2 differentiation of lymphocytes through the regulation of Il4 [38] , or M2 differentiation of macrophages through regulation of Il10 [39]. Our results are consistent with an anti-inflammatory role of Shh. We found for the first time that impaired Hh signalling in myoblasts promotes the expression of several Ccl chemokines. Our data confirms the role of Hh signalling as an essential regulator of tissue inflammation, and further demonstrates that Shh does not limit macrophage recruitment by signalling to macrophages directly or to ECs; but rather through the modulation of chemokine expression by myocytes (Figure 7).

In addition to providing evidence for the role of Shh in tissue homeostasis and regeneration in adults, this study further elucidates the process of regulation in ischemia-induced angiogenesis. Specifically, our data demonstrate that while increased macrophage recruitment in ischemic muscle accelerates angiogenesis; this increased angiogenesis is transient and does not lead to a long-term increase in tissue perfusion. Consistent with these results, a recent study demonstrated that administration of CD14+ macrophages in mice increases the number of perfused blood vessels both in an *in vivo* Matrigel plug assay and in the hind limb ischemia model in mice; however, the blood vessels formed in the CD14+ macrophage-treated mice remained large, leaky and unable to recruit pericytes. As a consequence, CD14+ macrophages induced pathologic rather than physiologic and persistent angiogenesis, which did not result in any improvement of limb perfusion 2 weeks after hind limb ischemia was induced [40]. While the study by Choi YE et al. used cultured human peripheral blood derived macrophages in immuno-deficient mice; our study confirms these results under "fully physiological" conditions. Notably the vascular phenotype, we observed in the ischemic muscle of Shh deficient mice which is associated with an increased macrophage-derived VEGFA, resembles that of tumour vasculature with a high density of poorly muscularized blood vessels that are inefficient at promoting tissue perfusion [41]. Accordingly, remodelling of the newly formed capillary network within the lower limb muscle has been recently suggested to be essential for efficient limb perfusion. Indeed, while capillary density within the ischemic lower limb muscle (tibialis anterior and extensor digitorum longus muscle) is at least as high as that of a healthy muscle 10-14 days after HLI surgery [10, 42], limb perfusion remains low: the ratio of blood flow within the ischemic muscle vs healthy muscle remains only 0.5). One of the proposed explanations for that is that the newly generated capillary network is poorly muscularized[42].

While phenotyping LysM-Cre; $Smo^{Flox/Flox}$ mice, we found that Hh signalling is active in macrophages. Macrophages are sensitive to autocrine production of Ihh or Dhh, but not Shh. Nevertheless, Hh ligands do not modulate phagocytosis or macrophage migration. Notably, monocyte/macrophages were previously shown to produce Ihh and Dhh [43], and macrophage derived-Ihh was shown to promote M2 differentiation of macrophages [43]. Moreover, we have shown that impaired Hh signalling in macrophages slows down angiogenesis and promotes capillary muscularization (data not shown). As discussed in the above paragraph, capillary muscularization which is a feature of newly formed capillary maturation is essential for their functionality and thus may be responsible for the significantly enhanced muscle perfusion observed in LysM-Cre; $Smo^{Flox/Flox}$ mice. However, the role of Hh signalling in macrophages in the setting of ischemia-induced angiogenesis needs to be further investigated. Of note, Shh is not likely the Hh ligand controlling macrophages behaviour. Indeed, while impaired Hh signalling in macrophages promote capillary muscularization, Shh deficiency decreases capillary muscularization. Notably, we have previously reported that Shh of which

expression is induced by PDGF-BB in SMCs, promotes capillary muscularization [22]. This previous report also explains why the percentage of smMHC positive vessel is significantly decreased in Shh iKO mice while it is not different from control mice, in HSA-Cre^{ERT2}; Smo$^{Flox/Flox}$ mice.

Finally, the present study reveals that endogenous Shh and ectopically administered N terminal-Shh act differently in the setting of ischemic skeletal muscle repair. One explanation for this might be that the bioavailability (i.e. expression profile and solubility) of the 2 sources of Shh are different, however further investigations are necessary to fully understand why exogenous N terminal-Shh is pro-angiogenic while endogenous Shh is not. What is known so far is that when administered ectopically, Shh promotes VEGFA expression in fibroblasts and subsequently angiogenesis, what we found in the present study is that impaired Shh signalling in myocytes promotes the recruitment of VEGFA-expressing macrophages leading to an overall increased VEGFA expression within the ischemic muscle. It should be noted that this is not the first study to report contradictory effects of Hh signalling on blood vessel biology, in the brain endogenous Hh signalling has been reported to promote blood brain barrier integrity [34] , while a recent study showed that brain tumour-derived Dhh contributed to enhanced vascular permeability [44].

5. Funding
This study was funded by the "Institut National de la Santé et de la Recherche Médicale" and by the University of Bordeaux.

6. Acknowledgments
We thank Jérôme Guignard, Annabel Reynaud, Myriam Petit-Roussel and Jérémie Teillon for their technical help. We thank Christelle Boullé for administrative assistance.
Cre^{ERT2} mice are licensed by GIE-CERBM (ICS-IGBMC).

6. Conflicts of interest
None

8. References

1. Losordo DW, Dimmeler S. Therapeutic angiogenesis and vasculogenesis for ischemic disease. Part I: angiogenic cytokines. *Circulation* 2004;**109**:2487-2491.
2. Roncalli J, Tongers J, Renault MA, Losordo DW. Biological approaches to ischemic tissue repair: gene- and cell-based strategies. *Expert Rev Cardiovasc Ther* 2008;**6**:653-668.
3. Katoh M. WNT signaling in stem cell biology and regenerative medicine. *Curr Drug Targets* 2008;**9**:565-570.
4. Sahlgren C, Lendahl U. Notch signaling and its integration with other signaling mechanisms. *Regen. Med* 2006;**1**:195-205.
5. Lavine KJ, Kovacs A, Ornitz DM. Hedgehog signaling is critical for maintenance of the adult coronary vasculature in mice. *J Clin Invest* 2008;**118**:2404-2414.
6. Pola R, Ling LE, Aprahamian TR, Barban E, Bosch-Marce M, Curry C, Corbley M, Kearney M, Isner JM, Losordo DW. Postnatal recapitulation of embryonic hedgehog pathway in response to skeletal muscle ischemia. *Circulation* 2003;**108**:479-485.
7. Pola R, Ling LE, Silver M, Corbley MJ, Kearney M, Blake Pepinsky R, Shapiro R, Taylor FR, Baker DP, Asahara T, Isner JM. The morphogen Sonic hedgehog is an indirect angiogenic agent upregulating two families of angiogenic growth factors. *Nat Med* 2001;**7**:706-711.

8. Kusano KF, Pola R, Murayama T, Curry C, Kawamoto A, Iwakura A, Shintani S, Ii M, Asai J, Tkebuchava T, Thorne T, Takenaka H, Aikawa R, Goukassian D, von Samson P, Hamada H, Yoon YS, Silver M, Eaton E, Ma H, Heyd L, Kearney M, Munger W, Porter JA, Kishore R, Losordo DW. Sonic hedgehog myocardial gene therapy: tissue repair through transient reconstitution of embryonic signaling. *Nat Med* 2005;**11**:1197-1204.
9. Maun HR, Wen X, Lingel A, de Sauvage FJ, Lazarus RA, Scales SJ, Hymowitz SG. Hedgehog pathway antagonist 5E1 binds hedgehog at the pseudo-active site. *J Biol Chem* 2010;**285**:26570-26580.
10. Renault MA, Chapouly C, Yao Q, Larrieu-Lahargue F, Vandierdonck S, Reynaud A, Petit M, Jaspard-Vinassa B, Belloc I, Traiffort E, Ruat M, Duplaa C, Couffinhal T, Desgranges C, Gadeau AP. Desert hedgehog promotes ischemia-induced angiogenesis by ensuring peripheral nerve survival. *Circ Res* 2013;**112**:762-770.
11. Dassule HR, Lewis P, Bei M, Maas R, McMahon AP. Sonic hedgehog regulates growth and morphogenesis of the tooth. *Development* 2000;**127**:4775-4785.
12. Long F, Zhang XM, Karp S, Yang Y, McMahon AP. Genetic manipulation of hedgehog signaling in the endochondral skeleton reveals a direct role in the regulation of chondrocyte proliferation. *Development* 2001;**128**:5099-5108.
13. Muzumdar MD, Tasic B, Miyamichi K, Li L, Luo L. A global double-fluorescent Cre reporter mouse. *Genesis* 2007;**45**:593-605.
14. Schuler M, Ali F, Metzger E, Chambon P, Metzger D. Temporally controlled targeted somatic mutagenesis in skeletal muscles of the mouse. *Genesis* 2005;**41**:165-170.
15. Clausen BE, Burkhardt C, Reith W, Renkawitz R, Forster I. Conditional gene targeting in macrophages and granulocytes using LysMcre mice. *Transgenic Res* 1999;**8**:265-277.
16. Hameyer D, Loonstra A, Eshkind L, Schmitt S, Antunes C, Groen A, Bindels E, Jonkers J, Krimpenfort P, Meuwissen R, Rijswijk L, Bex A, Berns A, Bockamp E. Toxicity of ligand-dependent Cre recombinases and generation of a conditional Cre deleter mouse allowing mosaic recombination in peripheral tissues. *Physiol Genomics* 2007;**31**:32-41.
17. Claxton S, Kostourou V, Jadeja S, Chambon P, Hodivala-Dilke K, Fruttiger M. Efficient, inducible Cre-recombinase activation in vascular endothelium. *Genesis* 2008;**46**:74-80.
18. Couffinhal T, Silver M, Zheng LP, Kearney M, Witzenbichler B, Isner JM. Mouse model of angiogenesis. *Am J Pathol* 1998;**152**:1667-1679.
19. Oses P, Renault MA, Chauvel R, Leroux L, Allieres C, Seguy B, Lamaziere JM, Dufourcq P, Couffinhal T, Duplaa C. Mapping 3-dimensional neovessel organization steps using micro-computed tomography in a murine model of hindlimb ischemia-brief report. *Arterioscler Thromb Vasc Biol* 2009;**29**:2090-2092.
20. Renault MA, Vandierdonck S, Chapouly C, Yu Y, Qin G, Metras A, Couffinhal T, Losordo DW, Yao Q, Reynaud A, Jaspard-Vinassa B, Belloc I, Desgranges C, Gadeau AP. Gli3 regulation of myogenesis is necessary for ischemia-induced angiogenesis. *Circ Res* 2013;**113**:1148-1158.
21. Roncalli J, Renault MA, Tongers J, Misener S, Thorne T, Kamide C, Jujo K, Tanaka T, Ii M, Klyachko E, Losordo DW. Sonic hedgehog-induced functional recovery after myocardial infarction is enhanced by AMD3100-mediated progenitor-cell mobilization. *J Am Coll Cardiol* 2011;**57**:2444-2452.
22. Yao Q, Renault MA, Chapouly C, Vandierdonck S, Belloc I, Jaspard-Vinassa B, Daniel-Lamaziere JM, Laffargue M, Merched A, Desgranges C, Gadeau AP. Sonic hedgehog mediates a novel pathway of PDGF-BB-dependent vessel maturation. *Blood* 2014;**123**:2429-2437.
23. Straface G, Aprahamian T, Flex A, Gaetani E, Biscetti F, Smith RC, Pecorini G, Pola E, Angelini F, Stigliano E, Castellot JJ, Jr., Losordo DW, Pola R. Sonic hedgehog regulates angiogenesis and myogenesis during post-natal skeletal muscle regeneration. *J Cell Mol Med* 2009;**13**:2424-2435.

24. Bijlsma MF, Leenders PJ, Janssen BJ, Peppelenbosch MP, Ten Cate H, Spek CA. Endogenous hedgehog expression contributes to myocardial ischemia-reperfusion-induced injury. *Exp Biol Med (Maywood, NJ* 2008;**233**:989-996.
25. Rowitch DH, B SJ, Lee SM, Flax JD, Snyder EY, McMahon AP. Sonic hedgehog regulates proliferation and inhibits differentiation of CNS precursor cells. *J Neurosci* 1999;**19**:8954-8965.
26. Chiang C, Litingtung Y, Lee E, Young KE, Corden JL, Westphal H, Beachy PA. Cyclopia and defective axial patterning in mice lacking Sonic hedgehog gene function. *Nature* 1996;**383**:407-413.
27. van Tuyl M, Groenman F, Wang J, Kuliszewski M, Liu J, Tibboel D, Post M. Angiogenic factors stimulate tubular branching morphogenesis of sonic hedgehog-deficient lungs. *Dev Biol* 2007;**303**:514-526.
28. Vokes SA, Yatskievych TA, Heimark RL, McMahon J, McMahon AP, Antin PB, Krieg PA. Hedgehog signaling is essential for endothelial tube formation during vasculogenesis. *Development* 2004;**131**:4371-4380.
29. Byrd N, Becker S, Maye P, Narasimhaiah R, St-Jacques B, Zhang X, McMahon J, McMahon A, Grabel L. Hedgehog is required for murine yolk sac angiogenesis. *Development* 2002;**129**:361-372.
30. Outram SV, Varas A, Pepicelli CV, Crompton T. Hedgehog signaling regulates differentiation from double-negative to double-positive thymocyte. *Immunity* 2000;**13**:187-197.
31. Shah DK, Hager-Theodorides AL, Outram SV, Ross SE, Varas A, Crompton T. Reduced thymocyte development in sonic hedgehog knockout embryos. *J Immunol* 2004;**172**:2296-2306.
32. Omenetti A, Syn WK, Jung Y, Francis H, Porrello A, Witek RP, Choi SS, Yang L, Mayo MJ, Gershwin ME, Alpini G, Diehl AM. Repair-related activation of hedgehog signaling promotes cholangiocyte chemokine production. *Hepatology (Baltimore, Md* 2009;**50**:518-527.
33. Syn WK, Oo YH, Pereira TA, Karaca GF, Jung Y, Omenetti A, Witek RP, Choi SS, Guy CD, Fearing CM, Teaberry V, Pereira FE, Adams DH, Diehl AM. Accumulation of natural killer T cells in progressive nonalcoholic fatty liver disease. *Hepatology (Baltimore, Md* 2010;**51**:1998-2007.
34. Alvarez JI, Dodelet-Devillers A, Kebir H, Ifergan I, Fabre PJ, Terouz S, Sabbagh M, Wosik K, Bourbonniere L, Bernard M, van Horssen J, de Vries HE, Charron F, Prat A. The Hedgehog pathway promotes blood-brain barrier integrity and CNS immune quiescence. *Science* 2011;**334**:1727-1731.
35. van Dop WA, Heijmans J, Buller NV, Snoek SA, Rosekrans SL, Wassenberg EA, van den Bergh Weerman MA, Lanske B, Clarke AR, Winton DJ, Wijgerde M, Offerhaus GJ, Hommes DW, Hardwick JC, de Jonge WJ, Biemond I, van den Brink GR. Loss of Indian Hedgehog activates multiple aspects of a wound healing response in the mouse intestine. *Gastroenterology* 2010;**139**:1665-1676, 1676 e1661-1610.
36. Zacharias WJ, Li X, Madison BB, Kretovich K, Kao JY, Merchant JL, Gumucio DL. Hedgehog is an anti-inflammatory epithelial signal for the intestinal lamina propria. *Gastroenterology* 2010;**138**:2368-2377, 2377 e2361-2364.
37. Schumacher MA, Donnelly JM, Engevik AC, Xiao C, Yang L, Kenny S, Varro A, Hollande F, Samuelson LC, Zavros Y. Gastric Sonic Hedgehog acts as a macrophage chemoattractant during the immune response to Helicobacter pylori. *Gastroenterology* 2012;**142**:1150-1159 e1156.
38. Furmanski AL, Saldana JI, Ono M, Sahni H, Paschalidis N, D'Acquisto F, Crompton T. Tissue-derived hedgehog proteins modulate Th differentiation and disease. *J Immunol* 2013;**190**:2641-2649.

39. Zhou X, Liu Z, Jang F, Xiang C, Li Y, He Y. Autocrine Sonic hedgehog attenuates inflammation in cerulein-induced acute pancreatitis in mice via upregulation of IL-10. *PloS one* 2012;**7**:e44121.
40. Choi YE, Cha YR, Lee KM, Kim HJ, Yoon CH. Proangiogenic cells enhanced persistent and physiologic neovascularization compared with macrophages. *Exp Mol Med* 2015;**47**:e186.
41. Carmeliet P, Jain RK. Principles and mechanisms of vessel normalization for cancer and other angiogenic diseases. *Nat Rev Drug Discov* 2011;**10**:417-427.
42. Arpino JM, Nong Z, Li F, Yin H, Ghonaim N, Milkovich S, Balint B, O'Neil C, Fraser GM, Goldman D, Ellis CG, Pickering JG. Four-Dimensional Microvascular Analysis Reveals That Regenerative Angiogenesis in Ischemic Muscle Produces a Flawed Microcirculation. *Circ Res* 2017;**120**:1453-1465.
43. Pereira TA, Xie G, Choi SS, Syn WK, Voieta I, Lu J, Chan IS, Swiderska M, Amaral KB, Antunes CM, Secor WE, Witek RP, Lambertucci JR, Pereira FL, Diehl AM. Macrophage-derived Hedgehog ligands promotes fibrogenic and angiogenic responses in human schistosomiasis mansoni. *Liver Int* 2013;**33**:149-161.
44. Azzi S, Treps L, Leclair HM, Ngo HM, Harford-Wright E, Gavard J. Desert Hedgehog/Patch2 Axis Contributes to Vascular Permeability and Angiogenesis in Glioblastoma. *Front Pharmacol* 2015;**6**:281.

9. Figures Legends

Figure 1: ***Shh deficiency leads to a transient increase in angiogenesis***. (**A**) Rosa26-Cre^{ERT2}; Rosa26^{mTmG} mice underwent HLI surgery and were sacrificed 10 days later. Cross sections of ischemic and non-ischemic tibialis anterior muscle were immuno-stained with anti-GFP antibodies (brown staining). (**B-D**) Rosa26-Cre^{ERT2}; Shh$^{Flox/Flox}$ mice (Shh iKO) and their control littermates (Shh$^{Flox/Flox}$ mice) underwent HLI surgery and were sacrificed 2 days later. (**B**) Shh, (**C**) Dhh and (**D**) Ihh mRNAs were quantified by real time RT PCR and normalized to HPRT mRNA both in the ischemic and non-ischemic tibialis anterior muscles (n=7 mice per group). (**E-H**) Rosa26-Cre^{ERT2}; Shh$^{Flox/Flox}$ mice (Shh iKO) and their control littermates (Shh$^{Flox/Flox}$ mice) underwent HLI surgery and were sacrificed 5 and 10 days later. (**E**) Ischemic tibialis anterior muscle cross sections were immuno-stained with anti-CD31 antibodies to identify blood vessels. Representative images of muscle sections from animals sacrificed 5 days after surgery are shown. (**F**) Capillary density was quantified as the number of CD31+ vessels per mm² (Day 5: n=7 control, n=6, Shh KO. Day 10 n=8 control, n=7, Shh KO). (**G**) Foot perfusion was measured via Laster Doppler Perfusion Imaging (LDPI). Representative perfusion images obtained 5 days after surgery are shown. (**H**) Blood flow was quantified as the ratio of blood flow in the ischemic foot versus non-ischemic foot 5 and 10 days after HLI surgery was performed (Day 5: n=10 control, n=10, Shh KO. Day 10 n=8 control, n=7, Shh KO). NI: not ischemic; I: ischemic; *: p<0.05; **: p<0.01, ***: p<0.001, NS: not significant, (**B**, **C**, **D**) One way ANOVA, (**F**,**H**) Mann-Whitney test.

Figure 2: **Ectopic administration of Shh does not rescue the phenotype of Shh deficient mice.** (**A-B**) 200 µg pIRES-NShh was administered in the ischemic tibialis anterior muscle of mice. (**A**) Muscle sections, harvested 6 days later, were stained with anti-Shh antibodies. (**B**) Shh protein expression was measured by western blot analysis at the indicated time points. (**C-F**) Rosa26-Cre^{ERT2}; Shh$^{Flox/Flox}$ mice (Shh iKO) and their control littermates (Shh$^{Flox/Flox}$ mice) underwent HLI surgery. Mice were intra-muscularly administered N-Shh-expressing or empty plasmids at day 0 and at day 4 (Day 5: n=10 control mice administered with empty plasmids, n=6 control mice administered with N-Shh expressing plasmids, n=9 Shh iKO mice administered with empty plasmids, n=5 Shh iKO mice administered with N-Shh expressing plasmids, Day 10: n=5 control mice administered with empty plasmids, n=7 control mice administered with N-Shh expressing plasmids, n=6 Shh iKO mice administered with empty plasmids, n=9 Shh iKO mice administered with N-Shh expressing plasmids). (**C-D**) Ischemic tibialis anterior muscle cross sections were immuno-stained with anti-CD31 antibodies to identify blood vessels. Capillary density was quantified as the number of CD31+ vessels par mm² (**C**) 5 and (**D**) 10 days after HLI was induced. (**E-F**) Blood flow was quantified as the ratio of blood flow in the ischemic foot versus not ischemic foot (**E**) 5 and (**F**) 10 days after HLI surgery was performed. *: p<0.05; NS: not significant, One way ANOVA.

Figure 3: ***Capillary muscularization is impaired in Shh deficient mice*.** (**A-B**) Rosa26-Cre^{ERT2}; Shh$^{Flox/Flox}$ mice (Shh iKO) and their control littermates (Shh$^{Flox/Flox}$ mice) underwent HLI surgery and were sacrificed 5 and 10 days later. (**A**) Ischemic muscle cross sections were co-immunostained with anti-smMHC antibodies (in red) to identify smooth muscle cells and anti-CD31 antibodies (in green) to identify ECs. Representative images of muscle sections from animals sacrificed 5 days after surgery are shown. (**B**) Blood vessel muscularization was quantified as the ratio of SmMHC+ vessels over CD31+ vessels (Day 5: n=7 control, n=11, Shh KO. Day 10 n=5 control, n=6, Shh KO). (**C-D**) Rosa26-Cre^{ERT2}; Shh$^{Flox/Flox}$ mice (Shh iKO) and their control littermates (Shh$^{Flox/Flox}$ mice) underwent HLI surgery and were sacrificed 5 days later. (**C**) The arterial network of mice was perfused post-mortem with a barium/latex mixture. (**D**) The number of collaterals was quantified (n=6 control, n=4, Shh iKO). (E) The diameter of collaterals was measured (n=18 control and 19 Shh iKO).*: p<0.05, NS: not significant, Mann-Whitney test.

Figure 4: ***Shh limits macrophage recruitment in the ischemic muscle*.** Rosa26-Cre^{ERT2}; Shh$^{Flox/Flox}$ mice (Shh iKO) and their control littermates (Shh$^{Flox/Flox}$ mice) underwent HLI surgery. (**A**-**C**) Mice were sacrificed 2 days later. (**A**) Ischemic tibialis anterior muscle cross sections were immuno-stained with anti-Ly6G (GR1) antibodies to identify neutrophils. (**B**) Neutrophil density was quantified as the number of GR1+ cells par mm² (n=6 control, n=8 Shh iKO). (**C**) Neutrophils infiltrated in the ischemic muscle were counted by FACS analysis using anti-Ly6G, Ly6C antibodies (n=9 control, n=4 Shh iKO). (**D**-**F**) Mice were sacrificed 5 and 10 days later. (**D**) Ischemic tibialis anterior muscle cross sections were immuno-stained with anti-CD68 antibodies to identify macrophages. Representative images of muscle sections from animals sacrificed 5 days after surgery are shown. (**E**) Macrophage density was quantified as the number of CD68+ cells par mm² (Day 5: n=8 control, n=6, Shh KO. Day 10 n=8 mice in each group). (**F**) Macrophages infiltrated in the ischemic muscle were counted by FACS analysis using anti-CD11c and anti-CD11b antibodies (n=7 control, n=10, Shh iKO). **: p<0.01, ***: p<0.001; NS: not significant, Mann-Whitney test.

Figure 5: ***Hyper inflammation is consequence of impaired Shh signalling to myocytes***. (**A**, **C**) HSA-Cre^{ERT2}; Smo$^{Flox/Flox}$ mice and their control littermates (Smo$^{Flox/Flox}$ mice) underwent HLI surgery and were sacrificed 5 and 10 days later. (**A**) Ischemic tibialis anterior muscle cross sections were immuno-stained with anti-CD68 antibodies to identify macrophages. Representative images of muscle sections from animals sacrificed 5 days after surgery are shown. (**B**) Macrophage density was quantified as the number of CD68+ cells per mm² (Day 5: n=10 control, n=12 HSA-Cre^{ERT2}; Smo$^{Flox/Flox}$. Day 10: n=7 control, n=13 HSA-Cre^{ERT2}; Smo$^{Flox/Flox}$). (**C**) Macrophages infiltrated in the ischemic muscle were double stained with anti-CD11c and anti-CD11b antibodies and counted by FACS analysis (n=9 control, n=16, HSA-Cre^{ERT2}; Smo$^{Flox/Flox}$). (**D**-**E**) C2C12 cells were treated with or without 30 nmol/L GDC-0449 for 24 hours. (**D**) Ccl2 and (**E**) Ccl5 mRNA expression level was quantified by real time RT-PCR and normalized to HPRT mRNA (n=6-9 per condition) (**F**-**H**) Myoblasts were isolated from Smo+/+ (control) and Smo$^{Flox/Flox}$ mice, and transduced with Cre expressing lentiviruses. (**F**) Smo, (**G**) Ccl2 and (**H**) Ccl5 mRNA expression level was quantified by real time RT-PCR and normalized to HPRT mRNA (n=8 per condition). (**I**) RAW 264.7 cells were seeded in the upper chamber of a Boyden chamber. The lower chamber contained myoblast-conditioned medium containing anti-Ccl2 antibodies of isotype control (n=9 per condition). *: p<0.05, **: p<0.01, ***: p<0.001, (B-H) Mann-Whitney test, (I) One way ANOVA.

Figure 6: ***Impaired Shh signalling to myocytes is sufficient to increase angiogenesis transiently***. HSA-Cre^{ERT2}; Smo$^{Flox/Flox}$ mice and their control littermates (Smo$^{Flox/Flox}$ mice) underwent HLI surgery and were sacrificed 5 and 10 days later. (**A**) Ischemic tibialis anterior muscle cross sections were immuno-stained with anti-CD31 antibodies to identify blood vessels. Representative images of muscle sections from animals sacrificed 5 days after surgery are shown. (**B**) Capillary density was quantified as the number of CD31 + vessels per mm² (Day 5: n=8 control, n=13 HSA-Cre^{ERT2}; Smo$^{Flox/Flox}$, day 10: n=6 control and n=11 HSA-Cre^{ERT2}; Smo$^{Flox/Flox}$). (**C**) Blood flow in the mice foot was evaluated by LDPI. Representative perfusion images obtained 10 days after surgery are shown. (**D**) Blood flow was quantified as the ratio of blood flow in the ischemic foot versus non-ischemic foot (Day 5: n=6 control, n=14 HSA-Cre^{ERT2}; Smo$^{Flox/Flox}$, day 10: n=8 control and n=11 HSA-Cre^{ERT2}; Smo$^{Flox/Flox}$). (**E**) Ischemic tibialis anterior muscle cross sections were co-stained with anti-VEGFA antibodies (in green) and anti-CD68 antibodies (in red). Representative images of muscle sections from animals sacrificed 5 days after surgery are shown. (**F**) VEGFA mRNA expression was quantified by real-time RT-PCR and normalized to HPRT mRNA in the ischemic tibialis anterior muscle of HSA-Cre^{ERT2}; Smo$^{Flox/Flox}$ mice and their control mice sacrificed 5 days after surgery (n=7 control, n=12 HSA-Cre^{ERT2}; Smo$^{Flox/Flox}$). *: p<0.05, **: p<0.01, NS: not significant. Mann-Whitney test.

Figure 7: **Schema representing the main events leading to a transient increase in angiogenesis in the absence of Shh**. Myocytes are represented as big plurinucleated red rectangle cells. Macrophages are represented as round orange cells and ECs as pink cells.

Figure 1

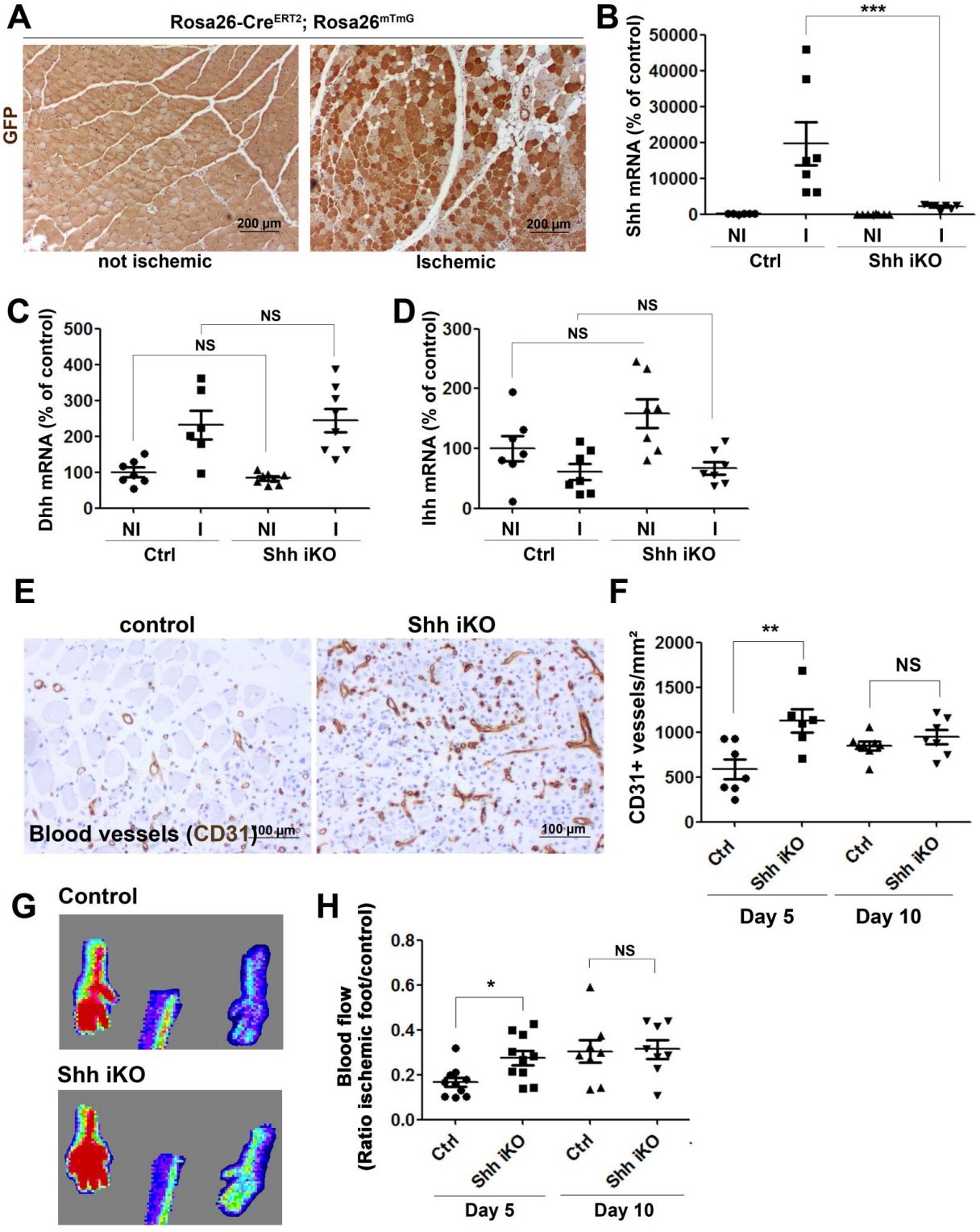
A
Rosa26-Cre^ERT2; Rosa26^mTmG
GFP
200 µm
200 µm
not ischemic
Ischemic
B
Shh mRNA (% of control)
***
NI
I
NI
I
Ctrl
Shh iKO
C
Dhh mRNA (% of control)
NS
NS
D
Ihh mRNA (% of control)
NS
NS
E
control
Shh iKO
Blood vessels (CD31)
100 µm
100 µm
F
CD31+ vessels/mm²
**
NS
Ctrl
Shh iKO
Ctrl
Shh iKO
Day 5
Day 10
G
Control
Shh iKO
H
Blood flow
(Ratio ischemic foot/control)
*
NS
Ctrl
Shh iKO
Ctrl
Shh iKO
Day 5
Day 10

Figure 2

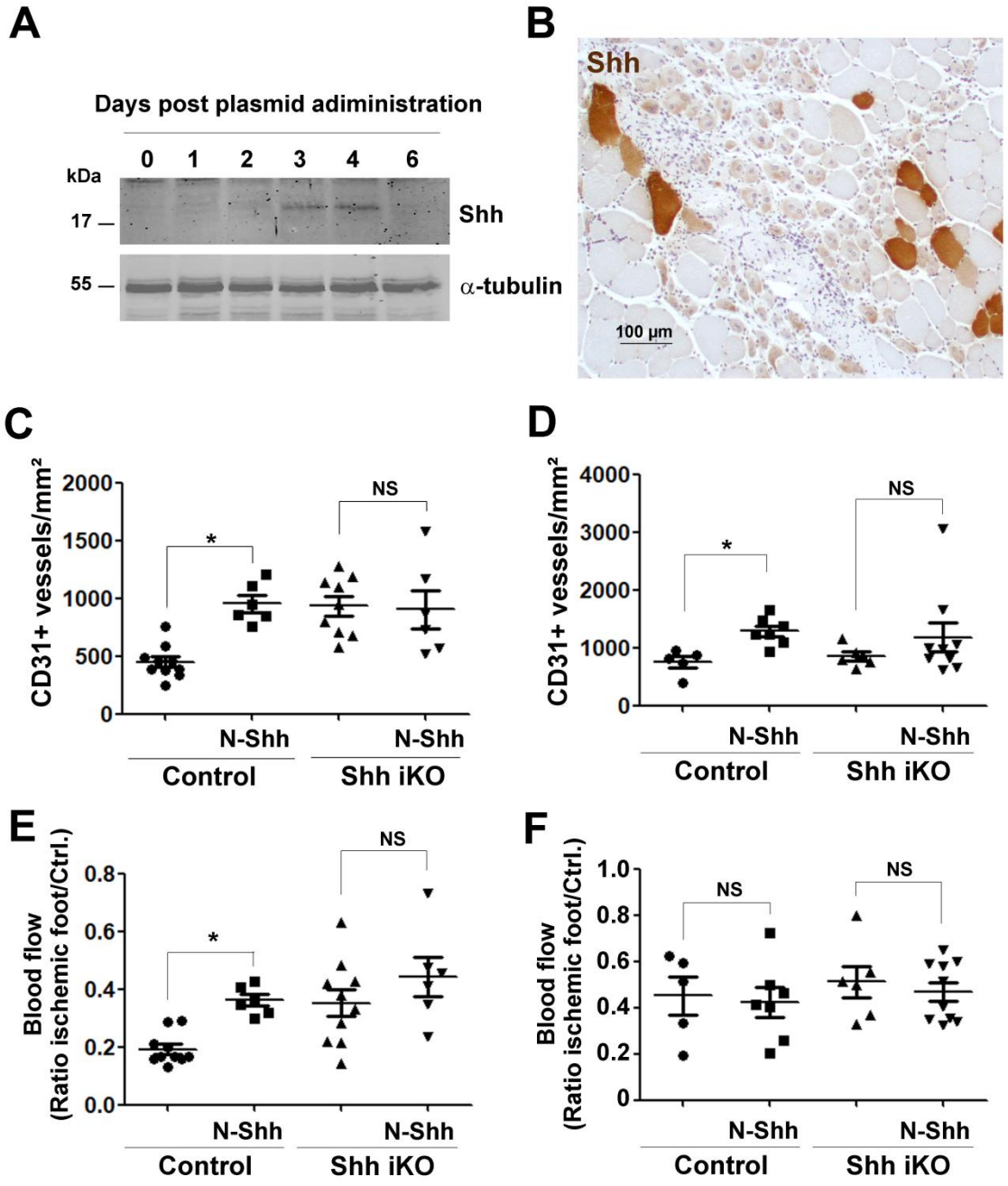
A
Days post plasmid adiministration
0 1 2 3 4 6
kDa
17
Shh
55
α-tubulin
B
Shh
100 µm
C
CD31+ vessels/mm²
2000
1500
1000
500
0
*
NS
N-Shh
N-Shh
Control
Shh iKO
D
CD31+ vessels/mm²
4000
3000
2000
1000
0
*
NS
N-Shh
N-Shh
Control
Shh iKO
E
Blood flow
(Ratio ischemic foot/Ctrl.)
0.8
0.6
0.4
0.2
0.0
*
NS
N-Shh
N-Shh
Control
Shh iKO
F
Blood flow
(Ratio ischemic foot/Ctrl.)
1.0
0.8
0.6
0.4
0.2
0
NS
NS
N-Shh
N-Shh
Control
Shh iKO

Figure 3

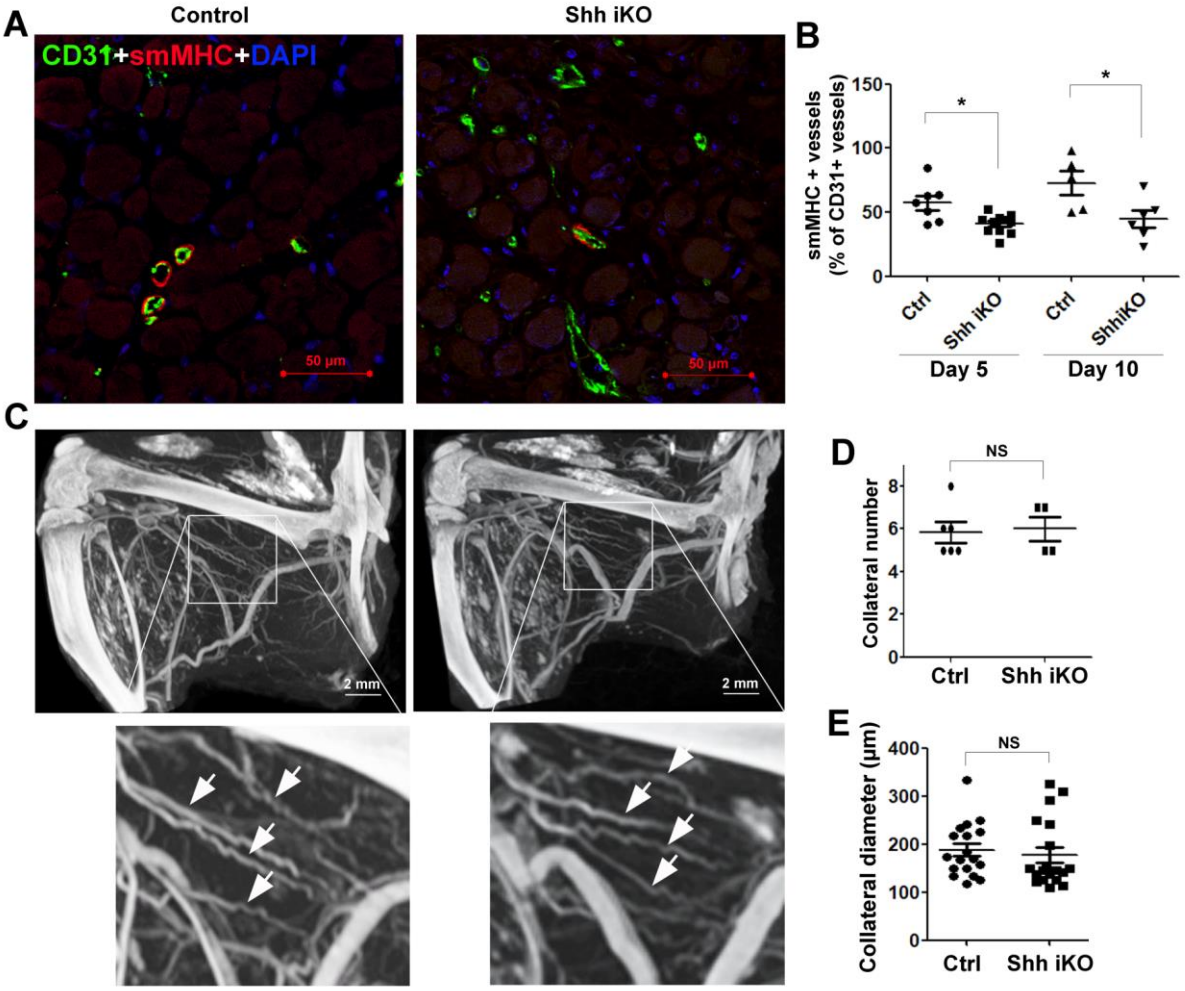
A
Control
Shh iKO
CD31+smMHC+DAPI
50 µm
50 µm
B
smMHC + vessels
(% of CD31+ vessels)
150
100
50
0
*
*
Ctrl
Shh iKO
Ctrl
ShhiKO
Day 5
Day 10
C
2 mm
2 mm
D
NS
Collateral number
8
6
4
2
0
Ctrl
Shh iKO
E
NS
Collateral diameter (µm)
400
300
200
100
0
Ctrl
Shh iKO

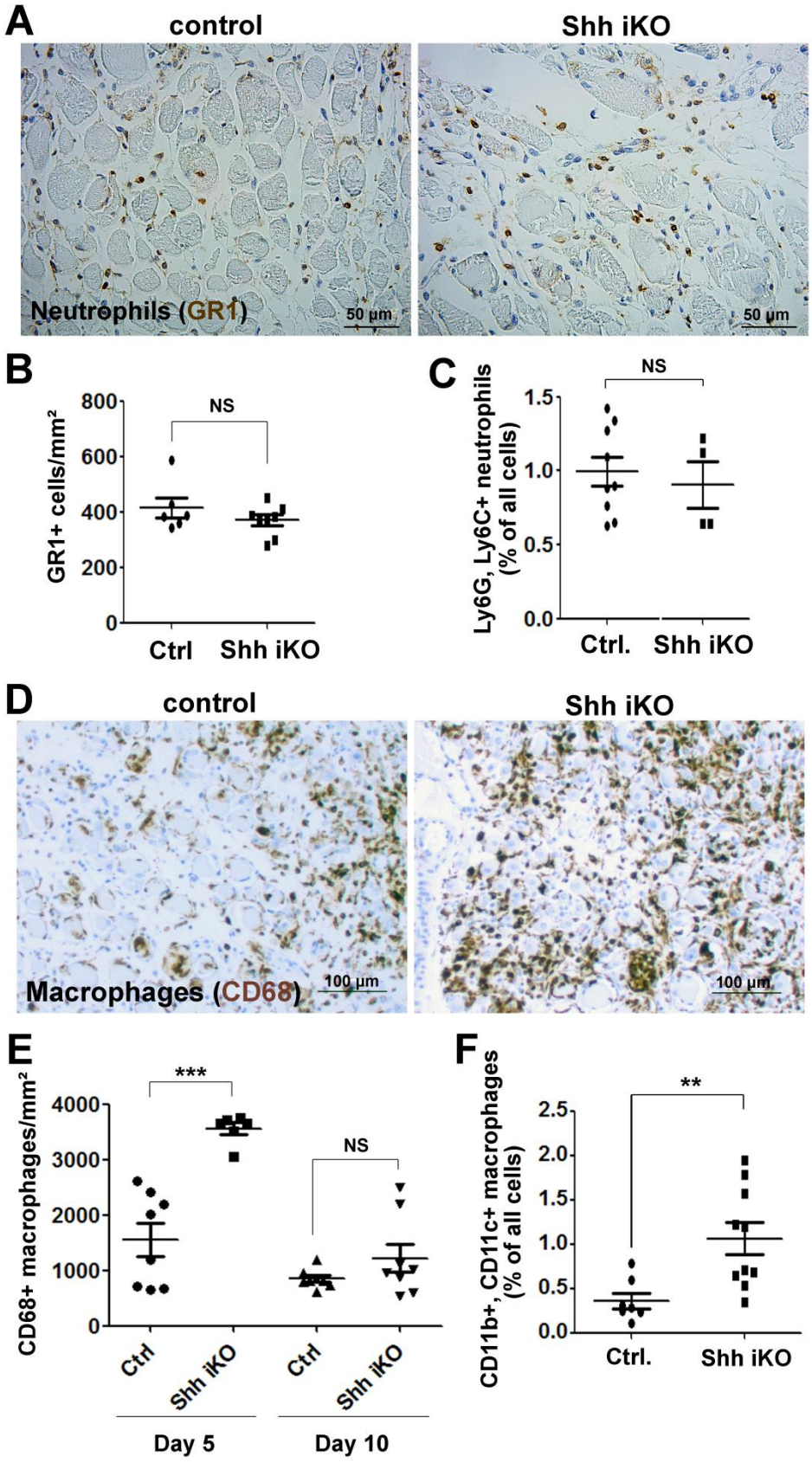
A
control
Shh iKO
Neutrophils (GR1)
50 µm
50 µm
B
GR1+ cells/mm²
800
600
400
200
0
NS
Ctrl
Shh iKO
C
Ly6G, Ly6C+ neutrophils (% of all cells)
1.5
1.0
0.5
0.0
NS
Ctrl.
Shh iKO
D
control
Shh iKO
Macrophages (CD68)
100 µm
100 µm
E
CD68+ macrophages/mm²
4000
3000
2000
1000
0
***
NS
Ctrl
Shh iKO
Ctrl
Shh iKO
Day 5
Day 10
F
CD11b+, CD11c+ macrophages (% of all cells)
2.5
2.0
1.5
1.0
0.5
0.0
**
Ctrl.
Shh iKO

Figure 4

Figure 5

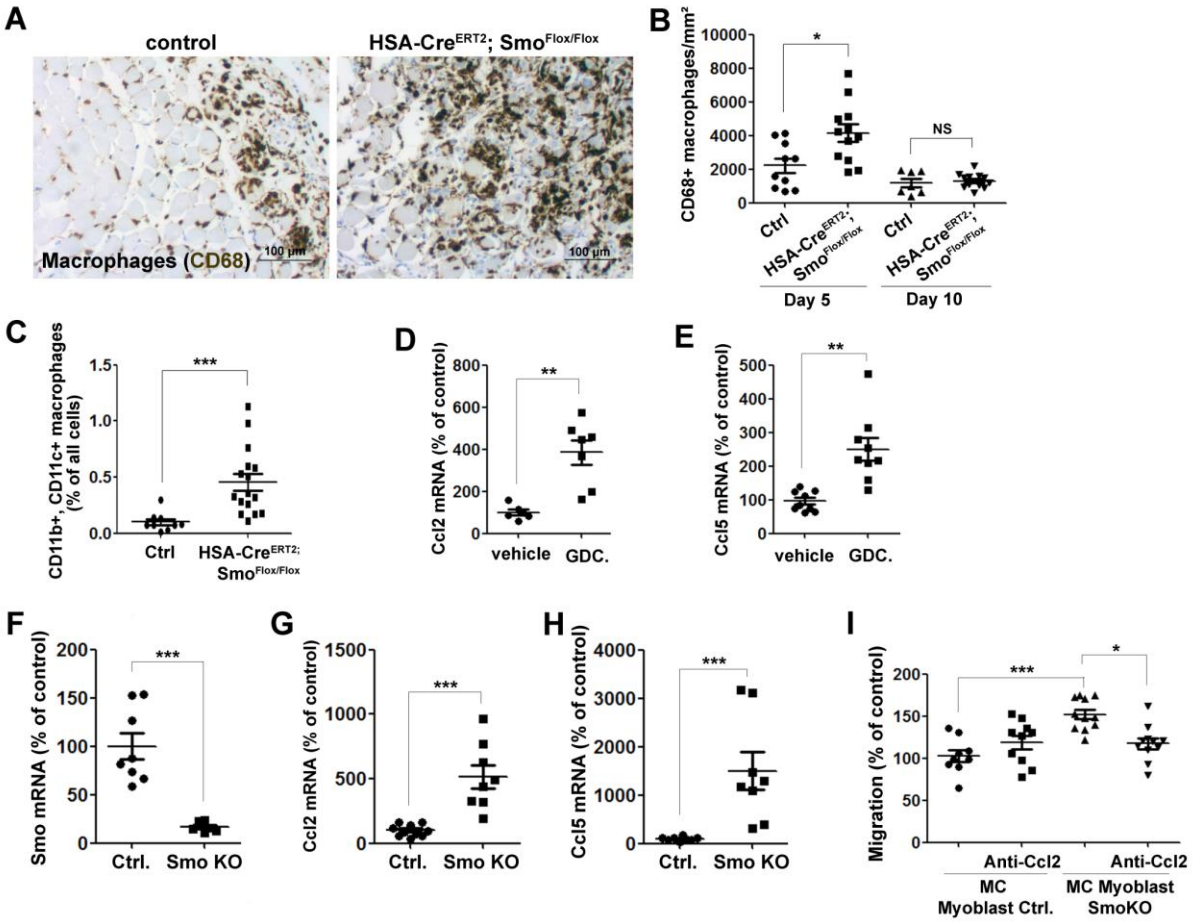
A
control
HSA-Cre^ERT2; Smo^Flox/Flox
Macrophages (CD68)
100 µm
B
CD68+ macrophages/mm²
Ctrl
HSA-Cre^ERT2; Smo^Flox/Flox
Day 5
Day 10
NS
C
CD11b+, CD11c+ macrophages (% of all cells)
Ctrl
HSA-Cre^ERT2; Smo^Flox/Flox
D
Ccl2 mRNA (% of control)
vehicle
GDC.
E
Ccl5 mRNA (% of control)
F
Smo mRNA (% of control)
Ctrl.
Smo KO
G
Ccl2 mRNA (% of control)
H
Ccl5 mRNA (% of control)
I
Migration (% of control)
Anti-Ccl2
MC Myoblast Ctrl.
MC Myoblast SmoKO

Figure 6

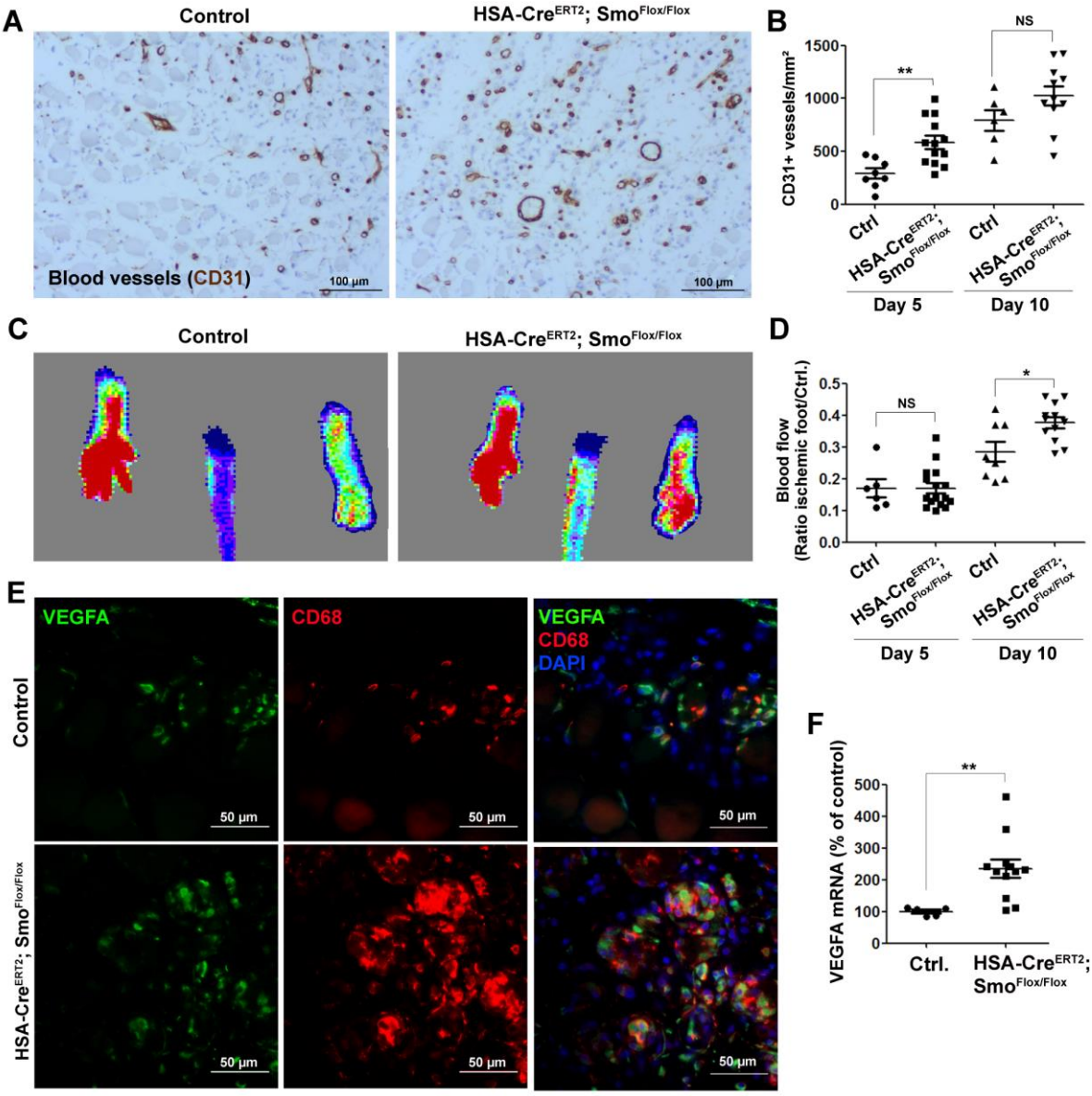
A
Control
HSA-Cre^ERT2; Smo^Flox/Flox
Blood vessels (CD31)
100 µm
B
CD31+ vessels/mm²
NS
**
Ctrl
HSA-Cre^ERT2; Smo^Flox/Flox
Day 5
Day 10
C
Control
HSA-Cre^ERT2; Smo^Flox/Flox
D
Blood flow (Ratio ischemic foot/Ctrl.)
NS
*
E
VEGFA
CD68
DAPI
Control
HSA-Cre^ERT2; Smo^Flox/Flox
50 µm
F
VEGFA mRNA (% of control)
**
Ctrl.
HSA-Cre^ERT2; Smo^Flox/Flox

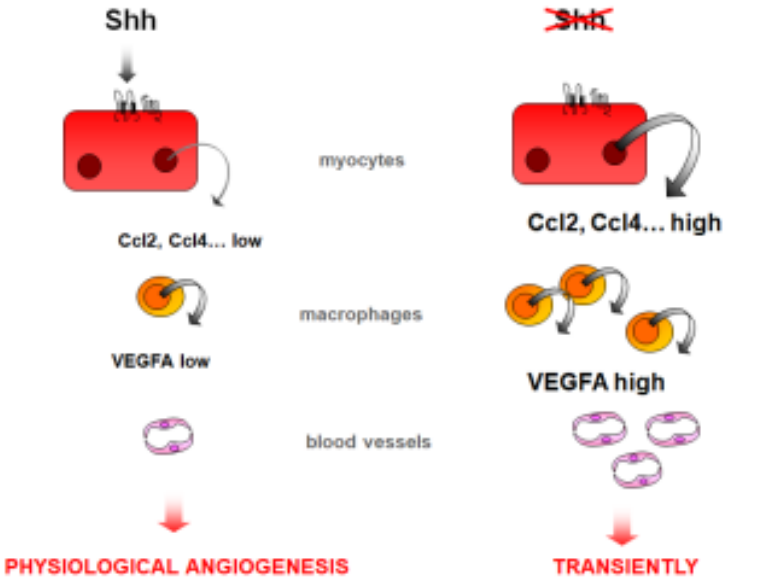
Shh
Shh
myocytes
Ccl2, Ccl4… low
Ccl2, Ccl4… high
macrophages
VEGFA low
VEGFA high
blood vessels
PHYSIOLOGICAL ANGIOGENESIS
TRANSIENTLY
INCREASED ANGIOGENESIS

Figure 7